Cypin: A novel target for traumatic brain injury

Przemyslaw Swiatkowski[a,b], Emily Sewell[d], Eric S. Sweet[a,c,1], Samantha Dickson[d], Rachel A. Swanson[a], Sara A. McEwan[a,c], Nicholas Cuccolo[a], Mark E. McDonnell[e], Mihir V. Patel[a,c], Nevin Varghese[f], Barclay Morrison[f], Allen B. Reitz[e], David F. Meaney[d], Bonnie L. Firestein[a,*]

[a] Department of Cell Biology and Neuroscience, Rutgers University, 604 Allison Road, Piscataway, NJ 08854-8082, USA
[b] Graduate Program in Molecular Biosciences, Rutgers University, 604 Allison Road, Piscataway, NJ 08854-8082, USA
[c] Graduate Program in Neurosciences, Rutgers University, 604 Allison Road, Piscataway, NJ 08854-8082, USA
[d] Department of Bioengineering, University of Pennsylvania, Philadelphia, PA 19104-6391, USA
[e] Fox Chase Chemical Diversity Center, Inc., Doylestown, PA 18902, USA
[f] Department of Biomedical Engineering, Columbia University, New York, NY 10027, USA

ARTICLE INFO

ABSTRACT

Cytosolic PSD-95 interactor (cypin), the primary guanine deaminase in the brain, plays key roles in shaping neuronal circuits and regulating neuronal survival. Despite this pervasive role in neuronal function, the ability for cypin activity to affect recovery from acute brain injury is unknown. A key barrier in identifying the role of cypin in neurological recovery is the absence of pharmacological tools to manipulate cypin activity *in vivo*. Here, we use a small molecule screen to identify two activators and one inhibitor of cypin's guanine deaminase activity. The primary screen identified compounds that change the initial rate of guanine deamination using a colorimetric assay, and secondary screens included the ability of the compounds to protect neurons from NMDA-induced injury and NMDA-induced decreases in frequency and amplitude of miniature excitatory postsynaptic currents. Hippocampal neurons pretreated with activators preserved electrophysiological function and survival after NMDA-induced injury *in vitro*, while pretreatment with the inhibitor did not. The effects of the activators were abolished when cypin was knocked down. Administering either cypin activator directly into the brain one hour after traumatic brain injury significantly reduced fear conditioning deficits 5 days after injury, while delivering the cypin inhibitor did not improve outcome after TBI. Together, these data demonstrate that cypin activation is a novel approach for improving outcome after TBI and may provide a new pathway for reducing the deficits associated with TBI in patients.

1. Introduction

Traumatic brain injury (TBI) is defined as brain dysfunction caused by an outside force applied to the head and is currently the leading cause of death for people under the age of 45 in the US. TBI is associated with disability, early-onset dementia, cognitive disorders, mental illness, and epilepsy (Nolan, 2005; Pearn et al., 2017; Prins et al., 2013). Nearly all of the approaches for treating TBI concentrate on protecting against neuronal degeneration, or alternatively, promoting neuronal survival (reviewed in (Werner and Stevens, 2015)). Although a common consequence of TBI is an alteration of neural circuits within injured brain regions, far fewer therapeutic approaches are designed to manipulate key molecules that shape neuronal circuits.

Although electrical stimulation of neural circuits offers one approach for repairing the brain after traumatic injury, these approaches do not offer a direct method to precisely target molecules that may actively reconstruct damaged circuits. One of the important ways that neuronal circuits are modified during neurological disease and injury is through synaptic plasticity and dendritic spine remodeling (Campbell et al., 2012a), which together affect neuronal connectivity (Han et al., 2014; Han et al., 2016; Han et al., 2015) and lead to adverse neuroplastic events (Tomaszczyk et al., 2014). Synaptic plasticity is a primary mechanism for remodeling neural circuits during learning acquisition and memory storage (Zucker and Regehr, 2002). At the structural level, plasticity can appear with enhancement or shrinkage of the dendritic spine (Lai and Ip, 2013) and an accompanying change to α-amino-3-

---

hydroxy-5-methyl-4-isoxazolepropionic acid (AMPA) receptor desensitization and localization (Otis et al., 1996; Kessels and Malinow, 2009) to these spines.

Cytosolic PSD-95 interactor (cypin) is a molecule that regulates plasticity by increasing dendrite number (Akum et al., 2004; Fernandez et al., 2008; O'Neill et al., 2015), decreasing dendritic spine density and maturity (Patel et al., 2018; Rodriguez et al., 2018), and increasing the frequency of miniature excitatory postsynaptic currents (Patel et al., 2018). At the circuit level, cypin overexpression results in an increase in spike count variability and a more complex distribution of spike waveforms (Rodriguez et al., 2018). Furthermore, overexpression of cypin confers resistance to *N*-methyl-D-aspartate (NMDA)-induced neuronal death, an *in vitro* model of secondary injury in TBI. As the major guanine deaminase in the brain (Akum et al., 2004; Fernandez et al., 2008; Patel et al., 2018; Firestein et al., 1999; Paletzki, 2002), cypin activates the first step of the purine salvage pathway to ultimately produce uric acid, an antioxidant that correlates with reduced damage after TBI (Hatefi et al., 2016; Adams et al., 2018), stroke (Yu et al., 1998; Romanos et al., 2007; Llull et al., 2016), and spinal cord injury (Scott et al., 2005; Du et al., 2007) and may decrease the development of neurological disorders, such as Parkinson's Disease (Alonso et al., 2007; De Vera et al., 2008). Additionally, cypin activity is important for proper brain development (Kumar and Rathi, 1976; Kumar et al., 1979) as the breakdown of guanine by cypin is necessary for the proper patterning of dendrites and formation of spines (Akum et al., 2004; Fernandez et al., 2008; Patel et al., 2018).

Guided by the role of cypin in regulating neural circuit function and producing antioxidants that may improve outcome after TBI, we chose an unexplored therapeutic approach of targeting cypin activity for treating TBI. We describe, for the first time, novel small molecules that modulate the effect of cypin on single cell electrophysiology, neuroprotection, and neuronal morphology. We further show the time course of change in cypin and its binding partner, postsynaptic density 95 (PSD-95), following CCI, and demonstrate that enhancing cypin's guanine deaminase activity with these novel small molecules will improve contextual memory in mice subjected to CCI.

2. Methods

2.1. Primary cortical neuron culture and injury

All animal studies were conducted in compliance with relevant local guidelines, such as the US Department of Health and Human Services Guide for the Care and Use of Laboratory Animals or MRC guidelines, and were approved by the Rutgers University, University of Pennsylvania, and Columbia University Institutional Animal Care and Use Committees. Neuronal cultures were plated from hippocampi of rat embryos at 18 days gestation on glass coverslips (12 mm diameter; 176,911 cells/cm^2 for electrophysiology and Sholl analysis, 47,244 cells/cm^2 for immunocytochemistry) previously coated with poly-D-lysine (Sigma-Aldrich) in full Neurobasal medium (Life Technologies, Grand Island, NY) supplemented with B-27 (Life Technologies) and GlutaMax (Life Technologies). At day *in vitro* (DIV) 7, cultures were transduced with pHUUG-GST-shRNA, pHUUG-Cypin-shRNA, GFP, or cypin overexpression lentiviral vectors, at DIV14 cultures were treated with 20 μM of each cypin modulator, and at DIV16 cultures were treated with NMDA in 0.1% DMSO for 5 min or vehicle, and allowed either 2 h of recovery before electrophysiological experiments, or 24 h before immunocytochemistry.

2.2. Drugs

N-methyl-D-aspartate (NMDA) was purchased from Sigma-Aldrich (St. Louis, MO). RAD001 and MK2206 were purchased from Selleckchem (Houston, TX). Dimethyl sulfoxide (DMSO) was purchased from Thermo Fisher Scientific (Waltham, MA). Small molecule cypin

modulators were selected and provided by Fox Chase Chemical Diversity Center, Inc. (Doylestown, PA).

2.3. COS-7 cell culture and transfection

COS-7 cells were plated at 70–80% confluence and maintained in Dulbecco's Modified Eagle Medium (DMEM) (Invitrogen), supplemented with 7.5% fetal bovine serum in a 5% CO$_2$ atmosphere. At 60% confluence, cells were transfected with 5 μg DNA using 7 μl Lipofectamine (Invitrogen) and Optimem (Invitrogen) using the manufacturer's protocol. Cells were left in Optimem for 12 h. After 12 h, a full media change in DMEM, penicillin/streptomycin and FBS (7.5%) was performed for each cell culture plate, and cells were grown for 24 h before protein was harvested for assay.

2.4. Guanine deaminase assay

The manufacturer's protocol for the Amplex Red Xanthine/Xanthine Oxidase Assay Kit (Invitrogen) was used to screen for presence of H$_2$O$_2$, a downstream product of guanine deaminase activity. Guanine (4 μl suspended at a concentration of 6.25 mM in 0.1 M NaOH) was added to the reaction mix (prepared as per manufacturer's instructions but for 2.5 ml total volume) to serve as the substrate for cypin. The product of this reaction, xanthine, can be measured readily by exciting the reactions at 530 nm and recording at 590 nm once/min at room temperature for 60 min in a 96 well plate format. A maximum of 48 wells were assayed at once to eliminate variability due to pipetting time. Cypin and control protein concentrations were measured by Bradford assay and normalized before each assay. GST proteins were aliquoted and stored at −80 °C while COS-7 cell-produced proteins were isolated fresh from culture the day of the assay. Guanine was suspended at 6.25 mM in 0.1 M NaOH and stored at −20 °C.

2.5. Definition of 1U of cypin in GDA assay

In consideration of the possible variability among batches of purified GST protein, we defined 1 unit (U) of enzymatic activity as the amount of cypin needed to create an absorbance change of 250 A/min in the presence of excess substrate. For all experiments performed with GST protein, 1U is equal to 22.5 pmol of GST-cypin. Changes in absorbance caused by cypin were conducted in the presence of 1000× greater concentration of guanine.

2.6. Preparation of proteins for use in GDA assay COS-7 cell lysate

Twenty four hours after COS-7 cell transfection with GFP-Cypin or GFP cDNA, cells were washed twice with phosphate-buffered saline (PBS) and scraped into 1 ml of GDA lysis buffer (150 mM NaCl, 25 mM Tris-HCl, pH 7.4 and 1 mM phenylmethane sulfonyl fluoride). Lysate was homogenized by passing it through a 25-gauge needle five times and was then centrifuged at 15,000 ×g at 4 °C for 10 min. Concentration of cytosolic proteins in the supernatant was measured using Bradford assay. At least nine replicates were performed for assay of the effects of each compound.

2.7. Dendrite analysis and imaging

We mixed cells from a rat expressing GFP under a universal promoter to obtain GFP-positive neurons with wildtype neurons at a ratio of 1:50 to obtain a culture that is appropriate for branching analysis (Fig. 3). Neurons were imaged in the GFP channel at 200× using an Olympus Optical IX50 microscope (Tokyo, Japan) with a Cooke Sensicam CCD cooled camera, fluorescence imaging system, and ImagePro software (MediaCybernetics, Silver Spring, MD). Dendrite morphology was digitized in three stages based on these initial images. In the first stage, the semi-automated tools available through the NeuronJ plugin

to ImageJ (NIH, Bethesda MD) were used to define coordinates of all dendrites in the x-y plane. In the second stage, NeuronStudio was used to define the pattern of connectivity between dendrites. These two steps fully determine the structure of each cell's dendritic arbor and encode it in a digital format. Custom scripts written in MATLAB (MathWorks, Natick, MA) converted the data from NeuronJ to NeuronStudio. Using these digitized dendritic arbors, a second set of MATLAB scripts was then used to analyze data and perform Sholl analysis with a 9.3 μm ring interval. The data were transferred to Excel for statistical analysis. The analyst was blinded to experimental conditions during all data analysis. Dendrites < 3 μm in length were not counted.

2.8. Western blot analysis

Mice were euthanized with an overdose of sodium pentobarbital. The brain was quickly removed and divided into cortical, hippocampal, and midbrain regions from the ipsilateral and contralateral hemispheres. Tissue was flash frozen for storage, and protein lysates were generated by re-suspending frozen tissue in TEE (25 mM Tris (pH 7.4), 1 mM EDTA, 1 mM EGTA) and RIPA lysis buffers (50 mM Tris (pH 7.4), 1% NP40, 0.25% sodium deoxycholate, 150 mM NaCl, 1 μM EDTA supplemented with protease and phosphatase inhibitors) at 4 °C for 1 h, and extracts were spun at 4 °C at $3000 \times g$ for 15 min to remove debris. Protein concentration was measured by a standard Bradford assay. Proteins (15 μg per sample) were resolved on a 10% SDS-poly-acrylamide gel and transferred to a polyvinylidene difluoride membrane. Membranes were blocked in 5% bovine serum albumin (BSA) in TBS-T (50 mM Tris, 150 mM NaCl, pH 7.6) for 1 h and incubated in primary antibodies diluted in blocking solution overnight at 4 °C. Membranes were then incubated for 1 h in secondary HRP-conjugated antibodies and subjected to HyGlo Western Blotting Detection System (Denville Scientific, Holliston, MA).

2.9. Immunocytochemistry

Cortical neurons were grown for 16 days in culture, and treated as previously described, on coverslips coated with poly-D-lysine. After immunostaining, coverslips were mounted on glass slides using Fluoromount G (Southern Biotechnology) and then imaged. Cultures were fixed in 4% paraformaldehyde in phosphate-buffered saline (PBS) for 10 min, permeabilized with 0.1% Triton X-100 in PBS + 5% normal goat serum, and immunostained with mouse anti-MAP2 (1:500) from Rockland and anti-GFP (1:500) from EMD Millipore followed by secondary antibodies conjugated to Alexa-Fluor® 488 (Invitrogen, 1:250) or Alexa-Fluor® 555 (Invitrogen, 1:250). Nuclei were stained with Hoechst 33,225 dye (1:1000). Neurons were visualized by immunofluorescence under a $10\times$ objective on an EVOS FL microscope. Only neurons positive for MAP2 immunostaining and Hoechst 33,225 staining were counted and used for statistical analysis.

2.10. Electrophysiology

Whole cell patch-clamp recordings were performed on the soma of cortical neurons. For recordings, cells were bathed in artificial cerebrospinal fluid containing (in mM): 140 NaCl, 5 KCl, 2 CaCl$_2$, 2 MgCl$_2$, 10 HEPES, and 10 glucose (pH 7.4 adjusted with NaOH; 290–310 mOsmol). Recording electrodes (3–5 MΩ) contained a K$^+$-based internal solution composed of (in mM): 126 K-gluconate, 4 KCl, 10 HEPES, 4 ATP−Mg, 0.3 GTP-Na$_2$, and 10 phosphocreatine (pH 7.2; 280–300 mOsmol). Miniature excitatory postsynaptic currents (mEPSCs) were recorded in presence of 1 μM tetrodotoxin (to block the action potentials) in the external solution, and 10 μM QX-314 (Tocris, R & D Systems; Minneapolis, MN) in the internal solution, GABA$_A$-mediated neurotransmission was blocked with 50 μM picrotoxin (Tocris, R & D Systems; Minneapolis, MN) as previously described. The membrane potential was held at -70 mV throughout all experiments. Data were

amplified and filtered at 2 kHz by a patch-clamp amplifier (Multiclamp 700B), digitalized (DIGIDATA 1440A), stored, and analyzed by pCLAMP (Molecular Devices; Union City, CA). Data were discarded when the input resistance changed > 20% during recording.

For long-term potentiation studies, hippocampal slices were cultured and recorded from as described in (Effgen et al., 2016; Vogel et al., 2016; Effgen et al., 2014). Briefly, hippocampi were dissected from brains of Sprague-Dawley rat pups aged P8-11. Hippocampi (400 μm thick slices) were cultured on porous Millipore Millicell cell culture inserts (Millipore, Billerica, MA) initially in Neurobasal medium supplemented with 1 mM L-glutamine, 1 x B27 supplement, 10 mM HEPES, and 25 mM D-glucose (Life Technologies, Grand Island, NY). Every 3 to 4 days, half of the medium was replaced with full-serum medium (FSM; 50% Minimum Essential Medium, 25% Hank's Balanced Salt Solution, 25% heat inactivated horse serum, 2 μM L-glutamine, 25 mM D-glucose, and 10 mM HEPES; Sigma, St. Louis, MO) for 10–12 days. All drugs were dissolved in DMSO to 20 μM and diluted in FSM at the indicated concentrations (a minimum of a 1:5000 DMSO:FSM ratio). Healthy cultures (< 5% propidium iodide staining, a marker for cell death) were transferred to FSM containing drugs for 48 h before testing for LTP induction. For LTP induction experiments, hippocampal slices were placed onto an 8×8 microelectrode array (MEA; Multi-Channel Systems, Reutlingen, Germany). Cultures were stimulated in the Schaffer collaterals (SC) at the current necessary to elicit a half-maximal response (I$_{50}$) once/min for 30 min to establish a stable baseline response. The slice was then stimulated (at I$_{50}$) with three 1 s 100 Hz pulse trains (with 1 s intervals) to induce LTP. Potentiation was then monitored by stimulating the SC at I$_{50}$ once/min for 60 min. The LTP induction was calculated as the percent difference between the average peak-to-peak amplitudes of the last 10 min of the post-stimulation and baseline recordings. For the drug treatment and control groups, seven to ten slices were studied.

2.11. Traumatic brain injury

All animal experiments were carried out in accordance with the National Institutes of Health guide for the care and use of Laboratory animals (NIH Publications No.8023, revised 1978). Adult male C57BL/6 mice (23-29 g) were anaesthetized with isoflurane (5% induction, 1–2% maintenance), placed in a stereotactic frame, and a 1.0 cm mid-line rostral-to-caudal incision was made to expose the skull. A craniotomy was performed over the left parietotemporal cortex midway between bregma and lambda sutures 2.5 mm lateral to the sagittal suture keeping the dura intact. One hour after induction of anesthesia, animals were placed under a compressed air controlled cortical impact (CCI) injury device. Mice were then subjected to a cortical impact brain injury. We used one of two impact conditions: 1) a mild cortical impact (1.0 mm depth, 0.4–0.5 m/s) that produces transient opening of the blood-brain barrier without hemorrhage, or 2) a moderate cortical impact (1.0 mm depth, 2.4–5.0 m/s), that creates a hemorrhagic contusion in the ipsilateral cortex. One hour following cortical impact brain injury, either drug or vehicle was injected directly into the ipsilateral hippocampus (X: -1.9, Y: 1.4, Z: -1.6; 200 μM drug concentration in aCSF vehicle; injected 1 μl over five minutes). Animals were either processed for immunohistochemistry, immunoblotting, or designated for neurobehavior testing. At various timepoints (24 h, 3 days, 7 days after injury), animals for immunohistochemistry were deeply anaesthetized with an overdose of sodium pentobarbital and transcardially perfused with 25 ml phosphate buffered saline followed by 25 ml of freshly hydrolysed 4% paraformaldehyde. Brains were removed, sectioned and stained with the appropriate antibodies. For immunoblotting, brains were quickly removed from euthanized animals and flash frozen. Animals for neurobehavior were analyzed 5 days post injury for deficits in fear conditioning, and brains were removed using fresh harvest procedures one week after injury.

a
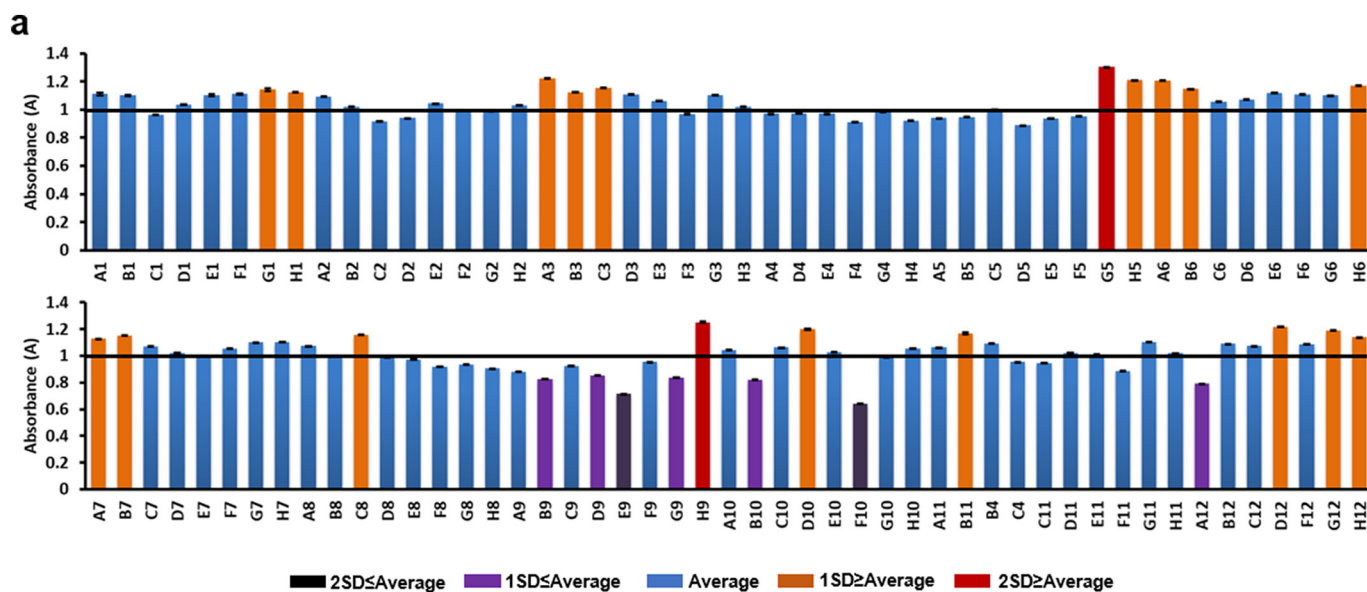
b

Common Name	Structure
H9	
B9	
G5	
G6	

Fig. 1. Small molecule compound screen for effects on cypin activity reveal discovery of both activators and inhibitors. (a) Lysate from COS-7 cells expressing GFP-cypin was used to assay and screen the effects of small molecule compounds on the guanine deaminase activity of cypin. Normalized slopes of the peak reaction velocity for guanine deaminase activity in the presence of the 96 compounds. Red bars denote reaction velocities two standard deviations above the normalized average of 1 ± 0.1185. Orange bars denote reaction velocities between one and two standard deviations above the normalized average. Blue bars denote reaction velocities within one standard deviation above or below the normalized average. Purple bars denote reaction velocities between one and two standard deviations below the normalized average. Black bars denote reaction velocities two standard deviations below the normalized average. (b) The structures of four compounds for further study. H9 and G5 are activators; B9 is an inhibitor; and G6 is a structurally-related inactive negative compound. Error bars indicate ± SEM. n ≥ 9 assays for each compound. (For interpretation of the references to colour in this figure legend, the reader is referred to the web version of this article.)

2.12. Fear conditioning

We evaluated the contextual fear conditioning response after CCI using procedures outlined previously (Patel et al., 2014). Four days following injury, mice were placed in a foot shock with sound attenuation for 2.5 min before three shocks (1 s duration, 100 mA) were delivered through the grid floor. Mice remained in the chamber for an additional 2.5 min following the shock stimulus. One day later, mice were returned to the test chamber and we recorded the animal movement over a five-minute span. Freezing behavior from the video footage was scored using an automated tracking algorithm we developed, which does not significantly differ from manual scoring methods. Freezing was defined as complete lack of animal movement for a period of at least 2 s (60 video frames). Fraction freezing time was defined as the percent of the total accumulated freeze time over the total recording time.

2.13. Statistics

Western blot, survival and electrophysiological data were analyzed for changes in treatment conditions when compared to control cells treated with vehicle or injured. Data were analyzed with ANOVA followed by Tukey-Kramer's multiple comparisons test using InStat and Prism software (GraphPad). p values < 0.05 were considered significant. Fear conditioning data was analyzed using a one way analysis of variance followed by Tukey's posthoc comparisons.

3. Results

We approached our examination of cypin as a therapeutic target for TBI in three distinct phases: we characterized the time course of changes to cypin and its binding partner PSD-95 after TBI, we identified small molecule activators and inhibitors of cypin and measured their effects on synaptic properties and neuronal survival after excitotoxicity, and we tested whether these novel compounds reverse the cognitive deficits in experimental TBI in mice.

3.1. Cypin and PSD-95 expression following TBI

Past work shows the controlled cortical impact (CCI) rodent model of TBI can elevate protein, neurotransmitter receptor, and neurotransmitter levels in the injured hemisphere, but these changes will depend on the injury severity (Chen et al., 2014; Hall et al., 2005; Osier and Dixon, 2016). To examine the possible contributions of cypin and PSD-95 across the TBI severity spectrum, we analyzed cortical and hippocampal brain tissue at 1, 7, and 14 days after mild or moderate injury for changes to these proteins. We observed a significant increase in cypin levels at 1 day post mild injury in ipsilateral and contralateral cortex, with no significant changes to cypin expression in the hippocampus (Supplementary Figs. 1, 2). There were no significant changes to PSD-95 expression levels following mild injury, while moderate injury led to an increase in PSD-95 at 1 day in the contralateral hippocampus (Supplementary Figs. 3, 4). These data indicate that the cypin-PSD-95 pathway may play a role after injury, suggesting its potential as a target for therapy.

3.2. Small molecule screen for cypin modulators

Our past work showed that increased cypin activity is neuroprotective (Tseng and Firestein, 2011). To discover small molecules that modulate the activity of cypin, we developed a screening platform that focused on measuring the relative level of guanine deaminase activity in COS-7 cells expressing cypin. We tested a select 288 member drug-like small molecule library that contains privileged scaffolds, such as piperazine, piperidine, and quinoline ring systems prevalent in CNS active therapeutics, and all met Linpinski guidelines for drug suitability.

A colorimetric guanine deaminase activity assay was used to screen this library for changes to activity in lysates from COS-7 cells expressing cypin. We normalized the activity levels of all compounds to an average initial rate of activity of 1 and identified multiple compounds that either increased or decreased the initial rate > 1 standard deviation (± 0.1185) from the average (Fig. 1).

To determine the appropriate concentration of the small molecules to use in future assays, we performed a concentration-effect study with one activator, H9 (1) (Supplementary Fig. 5). Treatment with H9 was not toxic to neurons at concentrations below 200 μM; however, at 200 μM, we observed 40% neuronal loss (Supplementary Fig. 5a,c). We also analyzed baseline response and ability to promote survival following NMDA-induced injury. Pretreatment with high concentrations of H9 had no beneficial effect following NMDA-induced injury, while concentrations of 1 μM and 10 μM significantly prevented neuronal loss (Supplementary Fig. 5a,c).

3.3. Cypin activator H9, but not G5, increases dendrite number

We have published extensively on the role of cypin in promoting dendritogenesis (Akum et al., 2004; Fernandez et al., 2008; O'Neill et al., 2015; Patel et al., 2018; Rodriguez et al., 2018); however, it is unclear what role the guanine deaminase activity plays in this activity (Akum et al., 2004; Patel et al., 2018). Thus, we tested the ability of inhibitor B9 and two cypin activators H9 and G5 to alter dendrite branching in hippocampal neurons. We selected the inhibitor B9 after excluding two additional inhibitors (E9, F10) since B9 also decreases the V_{max} of the reaction (data not shown). Simple quantitation revealed that only one of the activators, H9, significantly affected dendrite number; however, activator G5 and inhibitor B9 had no effect on dendrites (Supplementary Table 1). Furthermore, none of the compounds affected dendrite length (data not shown). These data suggest that in addition to increasing guanine deaminase activity, only H9 increases dendrites, consistent with our previous data that cypin's action on increasing dendritic arborization does not depend on guanine deaminase activity (Patel et al., 2018).

3.4. Cypin levels and activity play both pre- and postsynaptic roles in electrophysiological function

We previously reported that overexpression of cypin alters neuronal circuit synchrony (Rodriguez et al., 2018). However, the effects of cypin protein levels, and in turn, cypin activity on synaptic neurotransmission are still largely unknown. Here, we transduced rat primary hippocampal neurons at day *in vitro* 7 (DIV7) with lentivirus for GFP or cypin overexpression (Fig. 2a-c) or GST (control) or cypin knockdown (Fig. 2d-f) and recorded miniature excitatory postsynaptic currents (mEPSCs) at DIV14. Interestingly, cypin knockdown increased the amplitude of mEPSCs with no change to frequency, while neurons overexpressing cypin displayed increased frequency of mEPSCs with no change to amplitude. Knockdown of cypin also significantly shifted the cumulative probability curves for amplitude to the right (Fig. 2c,f). These data suggest that cypin plays both pre- and postsynaptic roles in the neuron and might be a target for modulation at both sites following injury.

3.5. Cypin activators reverse electrophysiological changes in neurons subjected to excitotoxic injury

To investigate whether cypin activators promote functional recovery following injury, we recorded mEPSCs following treatment. Neurons pretreated with H9 or G5 displayed no decrease in frequency or amplitude of mEPSCs that is normally observed after a 5 min NMDA-induced injury followed by 2 h recovery (Supplementary Fig. 6; Fig. 3g-i), suggesting that cypin activators protect against functional deficits. However, when cypin was knocked down using previously validated
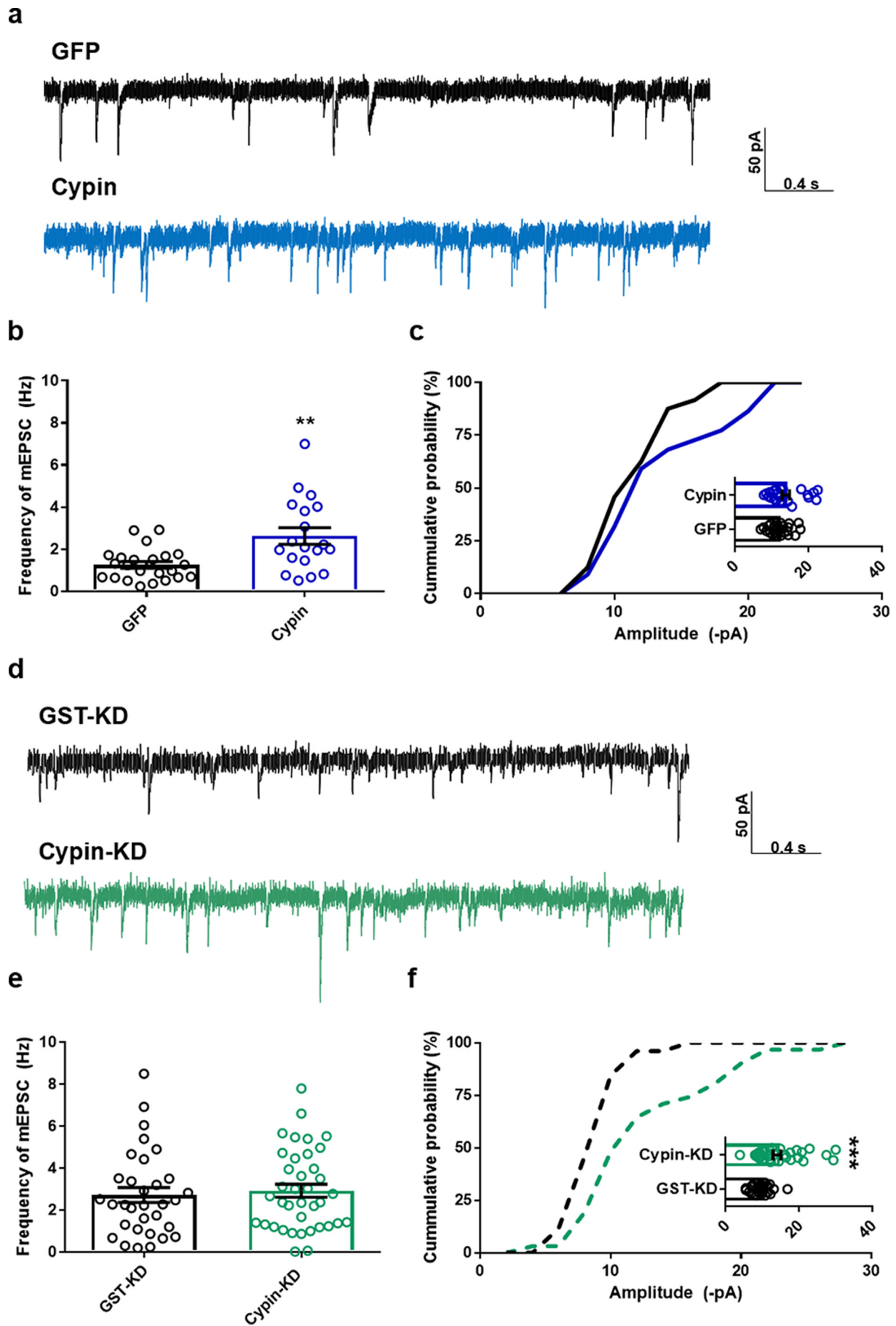
(caption on next page)

Fig. 2. Knockdown of cypin increases amplitude of mEPSCs, while overexpression of cypin increases frequency of mEPSCs. (a,d) Representative traces of mEPSCs. (b) Overexpression of cypin increases the frequency of mEPSCs (**p < 0.01). (c) The amplitude of mEPSCs remains unchanged after overexpression, with a slight right shift of the cumulative probability curve. Statistics calculated by one-way ANOVA followed by Tukey's multiple comparisons test (n = 26 for GFP, 22 for cypin). (e) Knockdown of cypin has no effect on frequency of mEPSCs when compared to GFP control. (f) Knockdown of cypin increases amplitude of mEPSCs when compared to GFP control and causes a right shift of the cumulative probability curve (***p < 0.005). Statistics calculated by one-way ANOVA followed by Tukey's multiple comparisons test (n = 17 for GFP, 21 for cypin knockdown).

shRNA (O'Neill et al., 2015; Tseng and Firestein, 2011; Chen and Firestein, 2007), H9 and G5 could not confer functional protection (Fig. 3j-l). Together, these data demonstrate that H9 and G5 require cypin for their mechanism of neuroprotection. Interestingly, treatment with H9 significantly increased the baseline frequency of mEPSCs in control neurons, and this effect was lost when cypin was knocked down (Fig. 3a-f). Consistent with the action of the activators, overexpression of cypin blocked decreases in mEPSC frequency and amplitude following injury (Fig. 4g-l).

When neurons overexpressing cypin were pretreated with B9, no protection from injury occurred (Fig. 4g-l), suggesting that the inhibitor counterbalanced the protective effects of overexpression. Furthermore, pretreatment of control neurons with H9 or G5 increased frequency of mEPSCs, consistent with cypin overexpression (Fig. 4a-f). In addition, pretreatment with neutral compound G6 had no effect on baseline or NMDA-induced decreases in mEPSCs (Figs. 3 and 4). Taken together, our data suggest that treatment with cypin activators act in the same manner as cypin overexpression and that cypin protein must be present for the activators to exert their effects. Since cypin plays pre- and postsynaptic roles in electrophysiological function (Figs. 2-4 and (Patel et al., 2018; Rodriguez et al., 2018)), we examined whether the small molecule activators, and hence cypin activity, could modulate long-term potentiation (LTP), the molecular mechanism underlying learning and memory. To test this, we used organotypic cultures of hippocampal slices and exposed the slices to the drugs at day *in vitro* 10, 11, or 12 for 48 h and conducted electrophysiology. In vehicle-treated slices, potentiation was approximately 40% in the CA1 region (Supplementary Fig. 7). Treatment with activators H9 and G5 had no effect on potentiation, while treatment with inhibitor B9 significantly blocked potentiation (10%; Supplementary Fig. 7). Furthermore, treatment with neutral compound G6 also had no effect on potentiation. These data suggest that cypin regulates normal synaptic function but does not affect LTP.

3.6. Cypin activators are neuroprotective in vitro

In the light of our previous report showing a neuroprotective function for cypin on neuronal survival in response to NMDA-induced injury (Tseng and Firestein, 2011), we next tested the small molecule compounds for their effects on neuronal survival following injury. NMDA exposure led to 50% survival at 24 h post-injury; pretreatment of cultures with H9 or G5 resulted in 100% survival after NMDA-induced injury. In comparison, neither B9 nor the neutral compound G6 had a neuroprotective effect (Supplementary Fig. 8), suggesting a neuroprotective function for cypin activation. Interestingly, treatment with B9 alone caused 25% neuronal death, demonstrating a detrimental effect of cypin inhibition (Supplementary Fig. 8; Fig. 5a, d, f, g). To examine if neuroprotection conferred from the compounds requires cypin, we again tested the compounds using neurons with cypin knocked down or overexpressed. Similar to published data (Tseng and Firestein, 2011), cypin knockdown reduces neuronal viability by approximately 75% (Fig. 5a, b) and blocks B9-induced neuronal death (Fig. 5a, e). Cypin knockdown leads to loss of neuroprotection from NMDA-induced injury by H9 and G5, suggesting that cypin is necessary for H9 and G5 action (Fig. 5h-j). As expected, cypin overexpression alone resulted in resistance to NMDA-induced neurotoxicity, and notably, this effect was blocked by B9 pretreatment (Fig. 5h, k, l), further supporting B9 inhibition of cypin activity. Expectedly, pretreatment with the neutral

compound G6 had no effect on survival (Fig. 5). Taken together, these data suggest that cypin plays a significant role in neuroprotective mechanisms following NMDA-induced injury and that the neuroprotective effect of H9 or G5 is dependent on action *via* cypin.

3.7. Cypin activators act to preserve neurobehavior after TBI in vivo

With this information on three separate compounds showing effects on electrophysiological function and neuronal viability following NMDA exposure, we took one final step and evaluated if the cypin activators H9 or G5 can promote functional recovery after TBI. We subjected animals to a moderate CCI, injected small molecule compounds directly into the hippocampus 1 h after injury, and tested fear conditioning response five days after injury. Without any treatment, mice showed a significant reduction in freeze percentage following TBI relative to sham surgical controls (p < 0.001), and this deficit was not significantly different from mice treated with an injection of drug vehicle (artificial cerebrospinal fluid (aCSF)) into the hippocampus (Fig. 6). Treatment with inhibitor B9 led to no improvement in freezing deficit when compared to vehicle-treated animals or untreated animals (p > 0.9, both comparisons; Fig. 6). However, treatment with cypin activators H9 or G5 significantly improved freeze percentage compared to untreated and vehicle-treated animals (p < 0.0001, H9 treated (injured) *vs* vehicle (injured); p < 0.0001, H9 treated (injured) *vs* untreated; p = 0.0022, G5 treated (injured) *vs* vehicle (injured); p = 0.0002, G5 treated (injured) *vs* untreated; Fig. 6a, b). For both H9 and G5 treatment, the injured and treated animals were not different from treatment only animals (H9, p > 0.9; G5, p > 0.55). Treatment with the cypin inhibitor B9 led to a significant impairment in sham animals (p < 0.0001 B9 *vs.* vehicle; p < 0.0001 B9 *vs.* untreated sham). Although mice treated with cypin activator H9 led to a slight, but significant, reduction in freeze percentage relative to sham and vehicle treated sham mice, treatment with the cypin activator G5 led to no significant impairment in either untreated sham or vehicle treated sham animals (p > 0.9, both comparisons). For G5 treatment, freeze percentage was not different between sham and injured animals (p = 0.55). Taken together, these data suggest that a single injection of cypin activator acutely after injury results in partial but significant recovery.

To determine whether the effects of the compounds *in vivo* could be due, in part, to changes in cypin and/or PSD-95 protein levels, we performed Western blot analysis on the cortices and hippocampi from the treated rats above. Treatment with H9, but not any other small molecule compound, resulted in elevated PSD-95 protein in the cortex at 1 day following injury (Supplementary Fig. 9). These alterations in PSD-95 levels following H9 treatment were not sustained at 7 or 14 days following moderate CCI (Supplementary Figs. 10–11). In comparison, none of the compounds led to significant changes to cypin at any timepoint for any drug treatment (Supplemental Figs. 9–11). These data suggest that the compounds most likely exert a neuroprotective effect *in vivo* independent of modulation of cypin and PSD-95 protein levels.

4. Discussion

Although it is well recognized that synaptic plasticity contributes to recovery after injury (Werner and Stevens, 2015), there are relatively few therapeutic approaches to directly target the activity of proteins
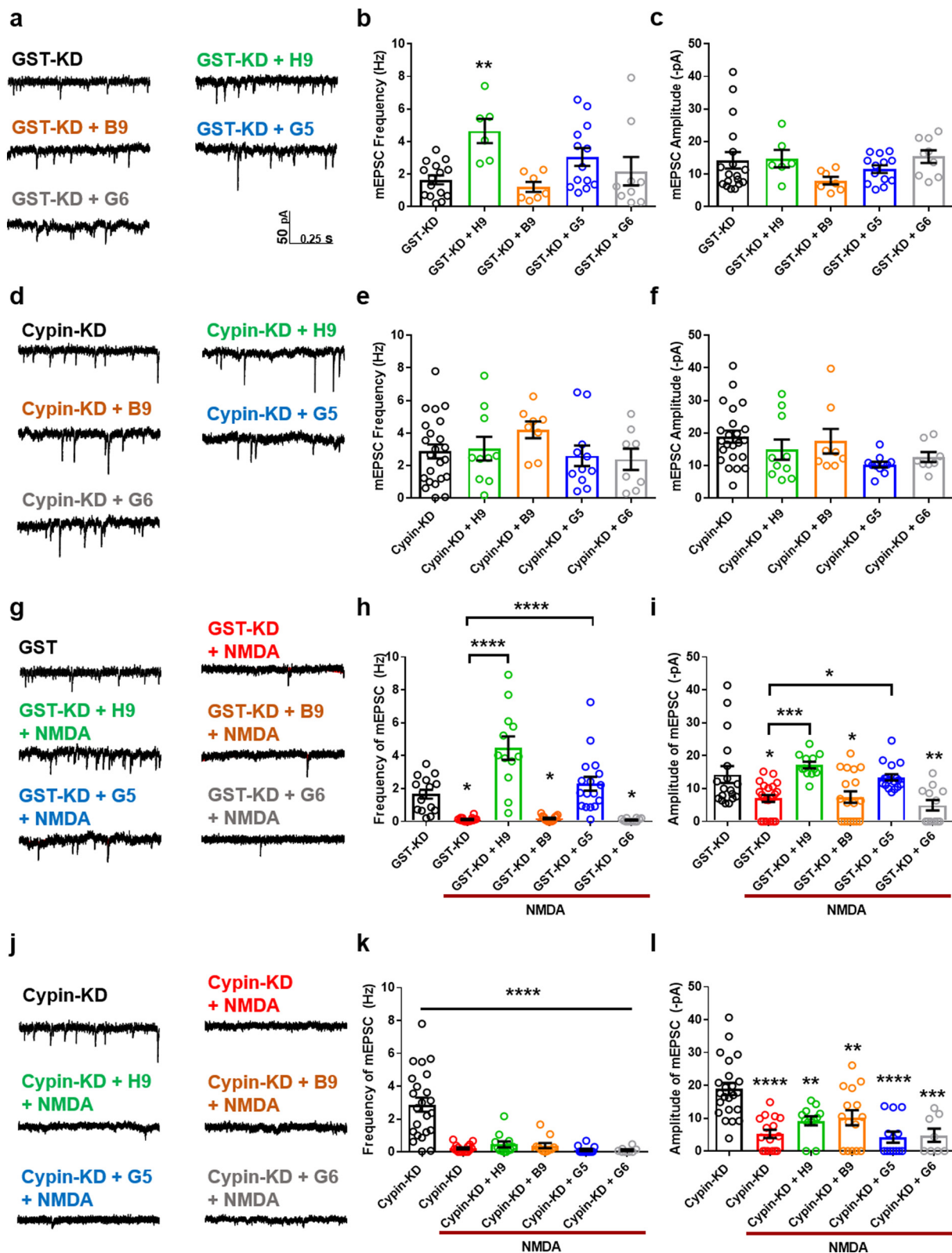
Fig. 3. The neuroprotective function of cypin activators is dependent on cypin expression. (a, d) Representative traces of mEPSCs recorded from control rat hippocampal neurons or neurons with cypin knockdown treated with vehicle (< 0.1% DMSO; control; n = 17/23) or 20 μM of the following compounds: H9, (n = 6/8), B9 (n = 7/8), G5 (n = 13/11), or G6 (n = 9/8). n = number of neurons/number of cultures. (b, c, e, f) Bar graph analysis of mEPSC frequency and amplitude following 48 h baseline drug treatment. Pretreatment with H9 increases the frequency of mEPSCs in control neurons with no change to amplitude. (g, j) Representative traces of mEPSCs recorded from rat hippocampal neurons treated with vehicle (< 0.1% DMSO; control; n = 17/23), or 20 μM of the following compounds: NMDA (n = 19/16), H9 + NMDA (n = 12/12), B9 + NMDA (n = 15/11), G5 + NMDA (n = 17/12), and G6 + NMDA (n = 12/8). n = number of neurons/number of cultures. (h,i,k,l) Bar graph analysis of mEPSC frequency and amplitude following 48 h drug treatment, 5 min 20 μM NMDA-induced injury, and two hour recovery period. Treatment with cypin activators prevents the decrease in frequency and amplitude induced by NMDA injury in control neurons, while cypin knockdown causes a loss of function and subsequent decrease of mEPSC frequency and amplitude. *p < 0.05, **p < 0.01, ***p < 0.005, ****p < 0.001 determined by one-way ANOVA followed by Tukey-Kramer multiple comparisons test. Error bars indicate mean ± SEM.
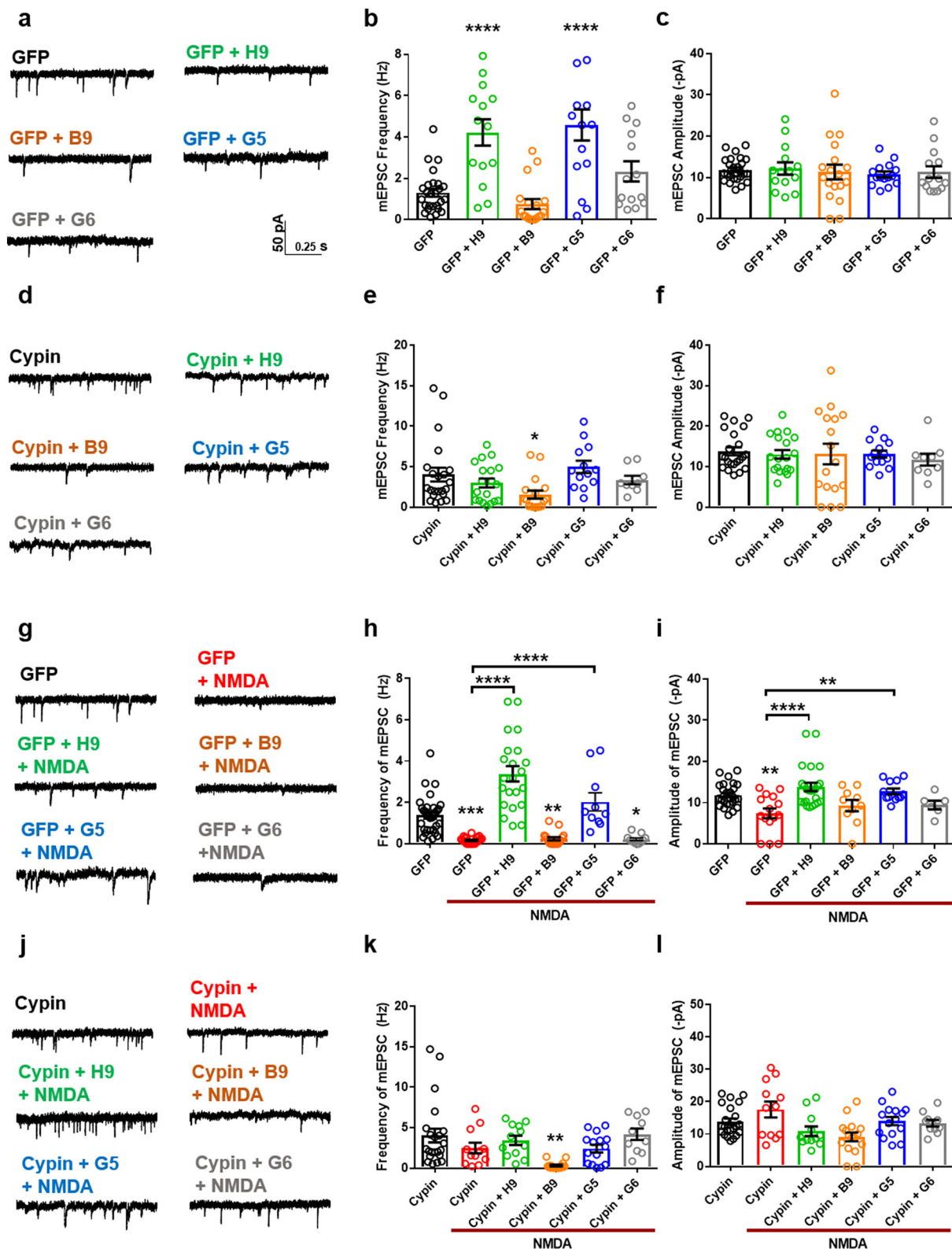
Fig. 4. Cypin overexpression prevents NMDA-induced injury. (a, d) Representative traces of mEPSCs recorded from rat hippocampal neurons overexpressing GFP (control) or cypin treated with vehicle (< 0.1% DMSO; control; n = 26/22) or 20 μM of the following compounds: H9, (n = 14/21), B9 (n = 18/17), G5 (n = 15/13), or G6 (n = 17/9). n = number of neurons/number of cultures. (b, c, e, f) Bar graph analysis of mEPSC frequency and amplitude following 48 h baseline drug treatment. H9 and G5 increased frequency of mEPSCs in control neurons with no change to amplitude. (g, j) Representative traces of mEPSCs recorded from rat hippocampal neurons treated with vehicle (< 0.1% DMSO; control; n = 32/22), or 20 μM of the following compounds: NMDA (n = 23/12), H9 + NMDA (n = 24/12), B9 + NMDA (n = 17/16), G5 + NMDA (n = 12/15), and G6 + NMDA (n = 11/10). n = number of neurons/number of cultures. (h, i, k, l) Bar graph analysis of mEPSC frequency and amplitude following 48 h drug treatment, 5 min 20 μM NMDA-induced injury, and two hour recovery period. Pretreatment with cypin activators prevents the decrease in frequency and amplitude induced by NMDA injury in control neurons, while cypin overexpression alone prevents the decrease of frequency and amplitude of mEPSCs, an effect blocked by pretreatment with B9. *$p < 0.05$, **$p < 0.01$, ***$p < 0.005$, ****$p < 0.001$ determined by one-way ANOVA followed by Tukey-Kramer multiple comparisons test. Error bars indicate ± SEM.
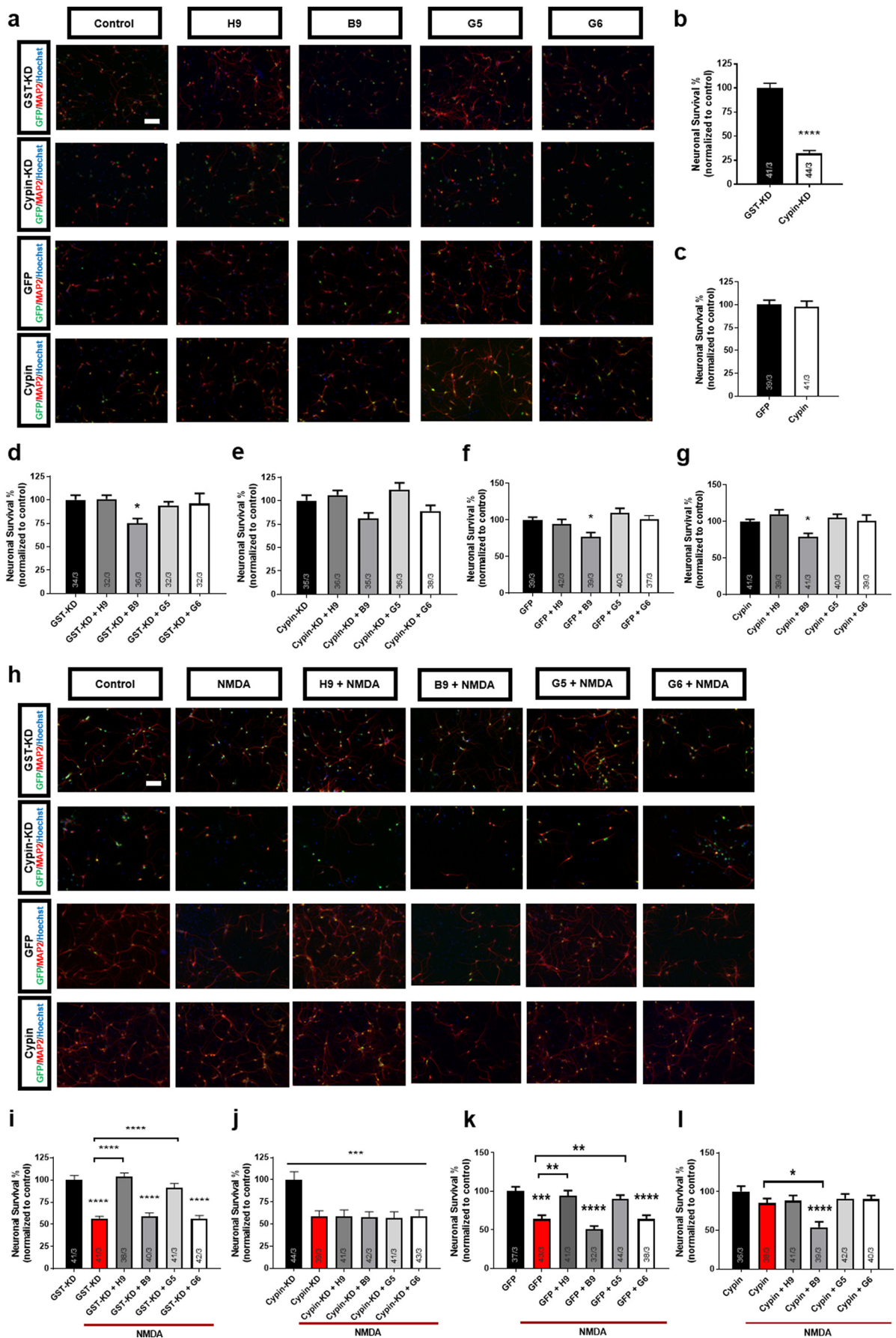
Fig. 5. Cypin knockdown abolishes neuroprotective activity of H9 and G5. (a) Representative images showing neurons immunostained for the neuronal marker, MAP2 and GFP and co-stained with nuclear dye, Hoechst 33225, after treatment with vehicle (0.1% DMSO; control), 20 μM NMDA, with or without 48 h pre-treatment with 20 μM H9, B9, G5, G6. Scale bar = 100 μm. (b-g). Quantitative analysis of neuronal survival expressed as percent live control neurons. Cypin activators, H9 and G5, prevent neuronal loss after injury, while the inhibitor, B9, and the neutral compound, G6, have no beneficial effect in control cultures. Cypin knockdown induces 75% cell death, and abolishes neuroprotective effects of H9 and G5. Data represent 39–43 samples from three separate trials. **$p < 0.01$, ***$p < 0.005$, ****$p < 0.001$ determined by one-way ANOVA followed by Tukey-Kramer multiple comparisons test. Error bars indicate ± SEM. (h) Representative images showing neurons immunostained for the neuronal marker, MAP2 and GFP, and co-stained with nuclear dye, Hoechst 33225, after treatment with vehicle (0.1% DMSO; control), 20 μM NMDA, with or without 48 h pretreatment with 20 μM H9, B9, G5, G6. Scale bar = 100 μm. (i-l). Quantitative analysis of neuronal survival expressed as percent live control neurons. Cypin activators, H9 and G5, prevent neuronal loss after injury, while the inhibitor, B9, and the neutral compound, G6, have no beneficial effect in control cultures. Cypin overexpression prevents neuronal death, and this effect is abolished by pretreatment with B9. Data represent 32–44 samples from three separate trials. *$p < 0.05$, **$p < 0.01$, ***$p < 0.005$, ****$p < 0.001$ determined by one-way ANOVA followed by Tukey-Kramer multiple comparisons test. Error bars indicate ± SEM.
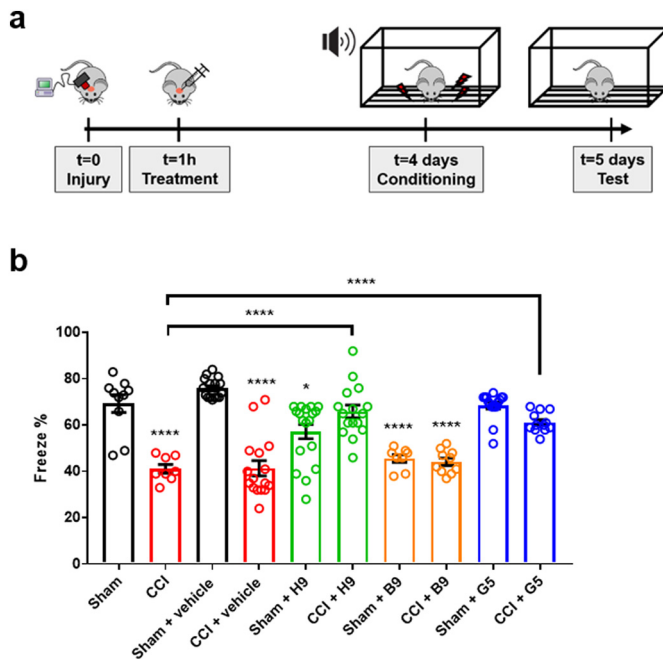
Fig. 6. Cypin activators H9 and G5 improve cognitive deficits after controlled cortical impact (CCI) model in mice. (a) Mice were subjected to CCI at day 0, followed by direct compound injections into the hippocampus at 1 h post-injury. After 4 days, mice were conditioned to the sound cue and foot shock, followed by testing on day 5. (b) Mice tested 5 days after CCI showed a significant decrease in freeze percentage measured during a fear conditioning test when compared to animals receiving a craniotomy, but no injury (sham). Inhibiting cypin (B9) led to a significant impairment in sham animals that was not significantly different from deficits in injured animals. In comparison, treating animals with cypin activators (H9, G5) led to a significant improvement in fear conditioning deficits in injured animals relative to both untreated and vehicle (aCSF) treated groups. Number of animals for each experimental group: sham = 10, CCI = 8, sham + vehicle = 16, CCI + vehicle = 16, sham + H9 = 18, CCI + H9 = 16, sham + B9 = 8, CCI + B9 = 10, sham + G5 = 16, CCI + G5 = 12. Select posthoc comparisons shown: **$p < 0.01$, ***$p < 0.005$, ****$p < 0.001$ determined by one-way ANOVA followed by Tukey-Kramer multiple comparisons test. Error bars indicate ± SEM.

that can play a role in rewiring damaged circuits. Among the therapeutic options, some focus on restoring cognitive function by reducing neuronal degeneration, while others are using cellular transplant strategies as either reconstructive technologies or cell-based platforms to deliver active biomolecules for the neural repair process (reviewed in (Werner and Stevens, 2015)). We now focus on identification of small molecule compounds that regulate cypin, the primary guanine deaminase in the brain (Akum et al., 2004; Fernandez et al., 2008; Firestein et al., 1999) that increases dendrite number (Akum et al., 2004; Fernandez et al., 2008), alters spine number (Patel et al., 2018; Rodriguez et al., 2018), decreases neuronal network bursting (Rodriguez et al., 2018; Chen et al., 2014) and regulates mESPC

frequency and amplitude (Patel et al., 2018). Building on our previously reported neuroprotective role for cypin (Tseng and Firestein, 2011) *in vitro*, we used an enzymatic screening assay to identify two novel compounds that enhance the guanine deaminase activity of cypin, protect neurons from NMDA-induced toxicity, and restore contextual memory after *in vivo* traumatic brain injury. Taken together, our results are the first to show the therapeutic potential of cypin activators for TBI treatment, and ours is the first study to demonstrate this role for cypin.

Past work targeting different synaptically localized molecules highlights the range of strategies available for restoring function after acute neurological injury. For example, PDS-95 is an important scaffolding molecule for spine stability and interacts with the carboxyl terminal of the NMDA receptor NR2B subunit to promote neuronal degeneration in response to excitotoxicity (Aarts et al., 2002; Sattler et al., 1999; Cui et al., 2007). Using peptides to interrupt the NMDA-PSD-95 interaction, and subsequently disrupt NMDA receptor signaling, rescues neurons in both *in vitro* and *in vivo* rodent models of ischemic damage (Aarts et al., 2002; Fan et al., 2010). Interrupting the NMDAR-PSD-95 interaction, however, may also adversely affect the interaction of PSD-95 with other synaptic proteins (Fernandez et al., 2009). Similarly, treatment of neuronal cultures with a peptide corresponding to the Ca^{2+} channel-binding domain on CRMP2 prevents NMDA-induced toxicity by reducing Ca^{2+} influx (Brittain et al., 2011), but the effects of this approach on neural circuits are not known. Similarly, it was reported that administration of edonerpic maleate, which binds to CRMP2, promotes motor function recovery after cryoinjury in the motor cortex in mice and after stroke in monkeys (Abe et al., 2018). Alternatively, blocking the calcium activated phosphatase calcineurin partially restores dendritic spine architecture after TBI (Campbell et al., 2012b), but this strategy also blocks the potentially beneficial effects of calcineurin on balancing synaptic strength (Wang and Kelly, 1996; Groth et al., 2003; Kim and Ziff, 2014). Cypin is an ideal target for the treatment of TBI as it acts on the microtubule cytoskeleton (Akum et al., 2004) to induce plasticity to both dendrites (Akum et al., 2004; Fernandez et al., 2008; O'Neill et al., 2015) and dendritic spines (Patel et al., 2018; Rodriguez et al., 2018), and the level of cypin expression influences pre- and postsynaptic mechanisms (Patel et al., 2018; Rodriguez et al., 2018) in a circuit. Unlike PSD-95, calcineurin, and CRMP2, cypin is the primary guanine deaminase in the brain (Firestein et al., 1999; Paletzki, 2002) and regulates brain uric acid levels, which is beneficial after injury induced by stroke in humans (Amaro et al., 2008; Logallo et al., 2011). Overexpression of cypin affects PSD-95 localization and another PSD-95-related protein SAP-102 (Firestein et al., 1999), and it regulates pre- and postsynaptic mechanisms (Patel et al., 2018; Rodriguez et al., 2018) whereas PSD-95 is a marker of postsynaptic sites (Cho et al., 1992). Thus, targeting cypin rather than synaptically localized proteins may be a more optimal approach for treatment after TBI (Toth, 2011).

In this work, we used multiple approaches to determine the function of cypin in healthy and injured neurons. We found that cypin overexpression increases the frequency of mEPSCs while knockdown increases the amplitude. These data suggest that cypin functions at both pre- and postsynaptic sites since frequency changes are generally

associated with neurotransmitter release probability from the presynaptic site, while changes in amplitude are explained by receptor composition at the postsynaptic site (Pinheiro, 2008). We previously reported that cypin binds zinc *via* His82, His84, His240, His279, and Asp330 residues (Fernandez et al., 2008). Zinc imbalance increases the amplitude of mEPSCs in a concentration-dependent manner and is likely to be involved in a number of psychiatric diseases, such as epilepsy, spreading depression, and ischemia (Lin et al., 2000; Toth, 2011; Zhu, 2012). It is possible that cypin knockdown leads to an increase in synaptic zinc, which may be responsible for the observed increase in mEPSC amplitude. Additionally, we previously reported that snapin binds to the CRMP homology domain of cypin *via* snapin's carboxyl-terminal coiled-coil domain, and overexpression of snapin decreases dendritic branching (Chen, 2005). At the presynaptic site, snapin binds to the SNARE complex *via* its interaction with SNAP-25 and increases binding of synaptotagmin to the SNARE complex following cAMP-dependent phosphorylation, effectively leading to vesicle exocytosis and neurotransmitter release (Vites et al., 2004). Studies investigating the effect of manipulation of snapin levels on neuronal electrophysiology and vesicle release dynamics show that snapin knockdown induces a decrease in mEPSC frequency and kinetics and a loss of homeostatic modulation of presynaptic vesicle release. In contrast, overexpression of a phosphomimetic mutant of snapin increases exocytosis in chromaffin cells (Vites et al., 2004). Based on our results, it is possible then that cypin increases trafficking of snapin to presynaptic sites, leading to increased vesicle priming and release, effectively increasing mEPSC frequency.

The activators that we identified in this study are N-benzoyl piperazines, and we are pursuing structure-function studies to further improve the affinity between the drug and its target, cypin. Our observations that cypin levels do not significantly decrease after trauma indicate that approaches to increase cypin enzymatic activity will not be limited by cypin availability over the first two weeks following trauma. Therefore, the intervention window for these small molecules may be wider than the one hour post-injury treatment that we used in this study. Morphological, electrophysiological, and behavioral analyses revealed that cypin activators do, indeed, prevent NMDA-induced injury *in vitro* and promote cognitive recovery following CCI, an effect not observed with the use of cypin inhibitor. Additionally, we show that the activators are dependent on the expression of cypin as cypin knockdown results in loss of neuroprotection. It is possible that these compounds act directly on cypin to increase GDA activity, promote dendrite branching, and decrease trafficking of PSD-95 or the related synapse-associated protein 102 (SAP-102) to the postsynaptic site (Chen, 2005). SAP-102 binds to the NMDA receptor NR2B subunit, which is highly permeable to calcium, a critical secondary messenger following secondary injury (Muller, 1996). Decreased trafficking of SAP-102 resulting from treatment with cypin activators may be one mechanism by which the observed neuroprotection and recovery of neuronal electrophysiology occur.

One limitation of our study is that our data do not clearly indicate how these compounds affect the guanine deaminase activity of cypin; possible mechanisms include that the molecules interfere with (activator) or promote binding to (inhibitor) a guanine deaminase inhibitor (Kumar et al., 1965; Kumar et al., 1967), which has been identified biochemically but not cloned. Alternatively, these molecules may interact directly with the guanine-binding site on cypin to alter its enzymatic activity. Regardless, our knockdown and overexpression studies show that the identified activators and inhibitor act only when cypin is present, strongly arguing against cypin-independent effects.

The novel activators and inhibitors of cypin enzymatic activity present new tools for studying other purine metabolic disorders with known neurological consequences. For example, patients with Lesch-Nyhan Syndrome (LNS) are deficient in hypoxanthine-guanine phosphoribosyltransferase (HPRT) (Lesch and Nyhan, 1964; Seegmiller et al., 1967), and show clear neurologic abnormalities. Even in patients with partial HPRT deficiency, cognitive deficits are present (Schretlen et al., 2001). As the deficiency in HPRT leads to higher levels of guanine, cypin will convert available guanine into xanthine, and eventually, uric acid blood levels rise and lead to gouty arthritis. In this condition, reducing the cypin activity may help restore normal uric acid levels. A number of cell culture studies support a role for purine metabolism in dendrite outgrowth and branching (Boer et al., 2001; Connolly et al., 2001) and neuronal differentiation (Yeh et al., 1998), pointing to additional opportunities for using these novel activators/ inhibitors for recovery after acquired neurological injuries (*e.g.*, stroke, posttraumatic epilepsy, traumatic spinal cord injury) and neurodegenerative disease (*e.g.*, Parkinson's Disease, Alzheimer's disease). Thus, molecules that modulate the guanine deaminase activity of cypin may have much broader utility for understanding a wide range of neurological diseases and disorders.

Taken together, our work shows that cypin plays a role in recovery after acute neurological injury and that the activation of cypin promotes neuronal survival and causes changes in synaptic electrophysiology that could explain the rebuilding of neural circuits after injury. The introduction of small molecules to alter the activity of cypin provides a new tool to explore the therapeutic value for controlling cypin activity after injury. Potentially valuable future studies include defining the therapeutic window for cypin after injury, the relative efficacy of these activators across different injury severities, and the continual refinement of the compounds to precisely determine their mechanism of action and improve their delivery across the blood-brain barrier. With these studies in place, we can develop new insights for promoting recovery after TBI and other neurological disorders.

Declaration of interest

Allen B. Reitz is a part owner of both ALS Biopharma, LLC and Fox Chase Chemical Diversity Center, Inc. Mark E. McDonnell is employed by Vironika, LLC and is also a part owner of Fox Chase Chemical Diversity Center, Inc. The remaining authors declare that they have no competing financial interests.

Appendix A. Supplementary data

Supplementary data to this article can be found online at https://doi.org/10.1016/j.nbd.2018.07.019.

References

Aarts, M., et al., 2002. Treatment of ischemic brain damage by perturbing NMDA receptor- PSD-95 protein interactions. Science 298, 846–850.

Abe, H., et al., 2018. CRMP2-binding compound, edonerpic maleate, accelerates motor function recovery from brain damage. Science 360, 50–57.

Adams, S.M., et al., 2018. ABCG2 c.421C > A is associated with outcomes after severe traumatic brain injury. J. Neurotrauma 35, 48–53.

Akum, B.F., et al., 2004. Cypin regulates dendrite patterning in hippocampal neurons by promoting microtubule assembly. Nat. Neurosci. 7, 145–152.

Alonso, A., Rodriguez, L.A., Logroscino, G., Hernan, M.A., 2007. Gout and risk of Parkinson disease: a prospective study. Neurology 69, 1696–1700.

Amaro, S., Planas, A.M., Chamorro, A., 2008. Uric acid administration in patients with acute stroke: a novel approach to neuroprotection. Expert. Rev. Neurother. 8, 259–270.

Boer, P., et al., 2001. Decelerated rate of dendrite outgrowth from dopaminergic neurons in primary cultures from brains of hypoxanthine phosphoribosyltransferase-deficient knockout mice. Neurosci. Lett. 303, 45–48.

Brittain, J.M., et al., 2011. Neuroprotection against traumatic brain injury by a peptide derived from the collapsin response mediator protein 2 (CRMP2). J. Biol. Chem. 286, 37778–37792.

Campbell, J.N., et al., 2012a. Mechanisms of dendritic spine remodeling in a rat model of traumatic brain injury. J. Neurotrauma 29, 218–234.

Campbell, J.N., Register, D., Churn, S.B., 2012b. Traumatic brain injury causes an FK506-sensitive loss and an overgrowth of dendritic spines in rat forebrain. J. Neurotrauma 29, 201–217.

Chen, M., 2005. A novel role for snapin in dendrite patterning: interaction with cypin. Mol. Biol. Cell 16, 5103–5114.

Chen, H., Firestein, B.L., 2007. RhoA regulates dendrite branching in hippocampal neurons by decreasing cypin protein levels. J. Neurosci. 27, 8378–8386.

Chen, Y., Mao, H., Yang, K.H., Abel, T., Meaney, D.F., 2014. A modified controlled cortical impact technique to model mild traumatic brain injury mechanics in mice. Front. Neurol. 5, 100.

Cho, K.O., Hunt, C.A., Kennedy, M.B., 1992. The rat brain postsynaptic density fraction contains a homolog of the Drosophila discs-large tumor suppressor protein. Neuron 9, 929–942.

Connolly, G.P., Duley, J.A., Stacey, N.C., 2001. Abnormal development of hypoxanthine-guanine phosphoribosyltransferase-deficient CNS neuroblastoma. Brain Res. 918, 20–27.

Cui, H., et al., 2007. PDZ protein interactions underlying NMDA receptor-mediated excitotoxicity and neuroprotection by PSD-95 inhibitors. J. Neurosci. 27, 9901–9915.

De Vera, M., et al., 2008. Gout and the risk of Parkinson's disease: a cohort study. Arthritis Rheum. 59, 1549–1554.

Du, Y., Chen, C.P., Tseng, C.Y., Eisenberg, Y., Firestein, B.L., 2007. Astroglia-mediated effects of uric acid to protect spinal cord neurons from glutamate toxicity. Glia 55, 463–472.

Effgen, G.B., et al., 2014. Isolated primary blast alters neuronal function with minimal cell death in organotypic hippocampal slice cultures. J. Neurotrauma 31, 1202–1210.

Effgen, G.B., et al., 2016. Primary blast exposure increases hippocampal vulnerability to subsequent exposure: reducing long-term potentiation. J. Neurotrauma 33, 1901–1912.

Fan, J., et al., 2010. N-methyl-D-aspartate receptor subunit- and neuronal-type dependence of excitotoxic signaling through post-synaptic density 95. J. Neurochem. 115, 1045–1056.

Fernandez, J.R., Welsh, W.J., Firestein, B.L., 2008. Structural characterization of the zinc binding domain in cytosolic PSD-95 interactor (cypin): role of zinc binding in guanine deamination and dendrite branching. Proteins 70, 873–881.

Fernandez, E., et al., 2009. Targeted tandem affinity purification of PSD-95 recovers core postsynaptic complexes and schizophrenia susceptibility proteins. Mol. Syst. Biol. 5, 269.

Firestein, B.L., Brenman, J.E., Aoki, C., Sanchez-Perez, A.M., 1999. El-Husseini, A. ED., Bredt, D.S. Cypin: a cytosolic regulator of PSD-95 postsynaptic targeting. Neuron 24, 659–672.

Groth, R.D., Dunbar, R.L., Mermelstein, P.G., 2003. Calcineurin regulation of neuronal plasticity. Biochem. Biophys. Res. Commun. 311, 1159–1171.

Hall, E.D., et al., 2005. Spatial and temporal characteristics of neurodegeneration after controlled cortical impact in mice: more than a focal brain injury. J. Neurotrauma 22, 252–265.

Han, K., et al., 2014. Disrupted modular organization of resting-state cortical functional connectivity in U.S. military personnel following concussive 'mild' blast-related traumatic brain injury. NeuroImage 84, 76–96.

Han, K., Chapman, S.B., Krawczyk, D.C., 2015. Altered amygdala connectivity in individuals with chronic traumatic brain injury and comorbid depressive symptoms. Front. Neurol. 6, 231.

Han, K., Chapman, S.B., Krawczyk, D.C., 2016. Disrupted intrinsic connectivity among default, dorsal attention, and Frontoparietal control networks in individuals with chronic traumatic brain injury. J. Int. Neuropsychol. Soc. 22, 263–279.

Hatefi, M., Dastjerdi, M.M., Ghiasi, B., Rahmani, A., 2016. Association of Serum Uric Acid Level with the severity of brain injury and Patient's outcome in severe traumatic brain injury. J. Clin. Diagn. Res. 10, OC20–OC24.

Kessels, H.W., Malinow, R., 2009. Synaptic AMPA receptor plasticity and behavior. Neuron 61, 340–350.

Kim, S., Ziff, E.B., 2014. Calcineurin mediates synaptic scaling via synaptic trafficking of Ca2+ −permeable AMPA receptors. PLoS Biol. 12, e1001900.

Kumar, S., Rathi, M., 1976. Deficiency of a naturally occurring protein inhibitor in brain of clinically 'brain damaged' newborn human infants - a possible cause of mental retardation? Neurosci. Lett. 3, 163–165.

Kumar, S., Tewari, K.K., Krishnan, P.S., 1965. Partial purification of guanine deaminase inhibitor from rat brain. J. Neurochem. 12, 1003–1004.

Kumar, S., Josan, V., Sanger, K.C., Tewari, K.K., Krishnan, P.S., 1967. Studies on guanine deaminase and its inhibitors in rat tissue. Biochem. J. 102, 691–704.

Kumar, S., Ou, S.W., Rathi, M., 1979. Deficiency of guanine deaminase in human brain: a new brain disorder? N. Engl. J. Med. 300, 1332–1333.

Lai, K.O., Ip, N.Y., 2013. Structural plasticity of dendritic spines: the underlying mechanisms and its dysregulation in brain disorders. Biochim. Biophys. Acta 1832, 2257–2263.

Lesch, M., Nyhan, W.L., 1964. A familial disorder of uric acid metabolism and central nervous system function. Am. J. Med. 36, 561–570.

Lin, D.D., Cohen, A.S., Coulter, D.A., 2000. Zinc-induced augmentation of excitatory synaptic currents and glutamate receptor responses in hippocampal CA3 neurons. Am. Physiol. Soc. 84, 2465–2476.

Llull, L., Amaro, S., Chamorro, A., 2016. Administration of Uric Acid in the emergency treatment of acute ischemic stroke. Curr. Neurol. Neurosci. Rep. 16, 4.

Logallo, N., et al., 2011. Serum Uri acid: neuroprotection in thrombolysis, The Bergen NORSTROKE study. BMC Neurol. 11, 114.

Muller, B.M., 1996. SAP102, a novel postsynaptic protein that interacts with NMDA receptor complexes in vivo. Neuron 17, 255–265.

Nolan, S., 2005. Traumatic brain injury a review. Crit. Care Nursing Quart. 28, 188–194.

O'Neill, K.M., et al., 2015. Assessing effects on dendritic arborization using novel Sholl analyses. Front. Cell. Neurosci. 9, 285.

Osier, N.D., Dixon, C.E., 2016. The controlled cortical impact model: applications, considerations for researchers, and future directions. Front. Neurol. 7, 134.

Otis, T., Zhang, S., Trussell, L.O., 1996. Direct measurement of AMPA receptor desensitization induced by glutamatergic synaptic transmission. J. Neurosci. 16, 7496–7504.

Paletzki, R.F., 2002. Cloning and characterization of guanine deaminase from mouse and rat brain. Neuroscience 109, 15–26.

Patel, T.P., et al., 2014. An open-source toolbox for automated phenotyping of mice in behavioral tasks. Front. Behav. Neurosci. 8, 349.

Patel, M.V., et al., 2018. A novel short isoform of cytosolic PSD-95 interactor (Cypin) regulates neuronal development. Mol. Neurobiol. 55 (8), 6269–6281.

Pearn, M.L., et al., 2017. Pathophysiology associated with traumatic brain injury: current treatments and potential novel therapeutics. Cell. Mol. Neurobiol. 37, 571–585.

Pinheiro, P.S.M., 2008. C. Presynaptic glutamate receptors: physiological functions and mechanisms of action. Nat. Rev. Neurosci. 9, 423–436.

Prins, M., Greco, T., Alexander, D., Giza, C.C., 2013. The pathophysiology of traumatic brain injury at a glance. Dis. Model. Mech. 6, 1307–1315.

Rodriguez, A.R., O'Neill, K.M., Swiatkowski, P., Patel, M.V., Firestein, B.L., 2018. Overexpression of cypin alters dendrite morphology, single neuron activity, and network properties via distinct mechanisms. J. Neural Eng. 15, 016020.

Romanos, E., Planas, A.M., Amaro, S., Chamorro, A., 2007. Uric acid reduces brain damage and improves the benefits of rt-PA in a rat model of thromboembolic stroke. J. Cereb. Blood Flow Metab. 27, 14–20.

Sattler, R., et al., 1999. Specific coupling of NMDA receptor activation to nitric oxide neurotoxicity by PSD-95 protein. Science 284, 1845–1848.

Schretlen, D.J., Harris, J.C., Park, K.S., Jinnah, H.A., del Pozo, N.O., 2001. Neurocognitive functioning in Lesch-Nyhan disease and partial hypoxanthine-guanine phosphoribosyltransferase deficiency. J. Int. Neuropsychol. Soc. 7, 805–812.

Scott, G.S., Cuzzocrea, S., Genovese, T., Koprowski, H., Hooper, D.C., 2005. Uric acid protects against secondary damage after spinal cord injury. Proc. Natl. Acad. Sci. U. S. A. 102, 3483–3488.

Seegmiller, J.E., Rosenbloom, F.M., Kelley, W.N., 1967. Enzyme defect associated with a sex-linked human neurological disorder and excessive purine synthesis. Science 155, 1682–1684.

Tomaszczyk, J.C., et al., 2014. Negative neuroplasticity in chronic traumatic brain injury and implications for neurorehabilitation. Neuropsychol. Rev. 24, 409–427.

Toth, K., 2011. Zinc in neurotransmission. Annu. Rev. Nutr. 31, 139–153.

Tseng, C.Y., Firestein, B.L., 2011. The role of PSD-95 and cypin in morphological changes in dendrites following sublethal NMDA exposure. J. Neurosci. 31, 15468–15480.

Vites, O.R.J., Schwarz, M., Rosenmund, C., Jahn, R., 2004. Reinvestigation of the role of snapin in neurotransmitter release. J. Biol. Chem. 279, 26251–26256.

Vogel, E.W., et al., 2016. Isolated primary blast inhibits long-term potentiation in Organotypic hippocampal slice cultures. J. Neurotrauma 33, 652–661.

Wang, J.H., Kelly, P.T., 1996. The balance between postsynaptic ca(2+)-dependent protein kinase and phosphatase activities controlling synaptic strength. Learn. Mem. 3, 170–181.

Werner, J.K., Stevens, R.D., 2015. Traumatic brain injury: recent advances in plasticity and regeneration. Curr. Opin. Neurol. 28, 565–573.

Yeh, J., Zheng, S., Howard, B.D., 1998. Impaired differentiation of HPRT-deficient dopaminergic neurons: a possible mechanism underlying neuronal dysfunction in Lesch-Nyhan syndrome. J. Neurosci. Res. 53, 78–85.

Yu, Z.F., Bruce-Keller, A.J., Goodman, Y., Mattson, M.P., 1998. Uric acid protects neurons against excitotoxic and metabolic insults in cell culture, and against focal ischemic brain injury in vivo. J. Neurosci. Res. 53, 613–625.

Zhu, J.E.A., 2012. Chronic zinc exposure decreases the surface expression of NR2A-containing NMDA receptors in cultured hippocampal neurons. PLoS One 7.

Zucker, R.S., Regehr, W.G., 2002. Short-term synaptic plasticity. Annu. Rev. Physiol. 64, 355–405.